JACS
JOURNAL OF THE AMERICAN CHEMICAL SOCIETY

ARTICLE

pubs.acs.org/JACS

Integration of Catalysis and Analysis is the Key: Rapid and Precise Investigation of the Catalytic Asymmetric Gosteli−Claisen Rearrangement

Johannes Troendlin,[†] Julia Rehbein,[‡] Martin Hiersemann,[‡] and Oliver Trapp*[,†]

[†]Organisch-Chemisches Institut, Ruprecht-Karls Universität Heidelberg, 69120 Heidelberg, Germany

[‡]Fakultät Chemie, Technische Universität Dortmund, 44227 Dortmund, Germany

Supporting Information

ABSTRACT: The kinetics of the Cu^{II}(bisoxazoline)-catalyzed diastereo- and enantioselective Gosteli−Claisen rearrangement of 2-alkoxycarbonyl-substituted allyl vinyl ethers has been investigated by enantioselective on-column reaction gas chromatography (ocRGC). Enantioselective ocRGC integrates (stereoselective) catalysis and enantioselective chromatography in a single microcapillary, which is installed in a GC-MS for direct analysis of conversion and selectivity. Thus, this technique allows direct differentiation of thermal and stereoselectively catalyzed reaction pathways and determination of activation parameters and selectivities of the individual reaction pathways starting from stereoisomeric reactants with high precision. Two modes of operation of enantioselective ocRGC are presented to investigate noncatalyzed, i.e., conversion of isopropyl-2-(allyloxy)but-2*Z*-enoate **1** to isopropyl-3*R*,*S*-methyl-2-oxy-hex-5-enoate (±)-**2** and the [Cu{(*R*,*R*)-Ph-box}](SbF$_6$)$_2$-catalyzed Gosteli−Claisen rearrangement, i.e., conversion of isopropyl-2-(but-2′*E*-en-1-yloxy)but-2*Z*-enoate (*E*,*Z*)-**3** to isopropyl-3*S*,4*S*-dimethyl-2-oxy-hex-5-enoate **4b**. Eyring activation parameters have been determined by temperature-dependent measurements: Uncatalyzed rearrangement of **1** to (±)-**2** gives $\Delta G^{\ddagger}$ (298 K) = 114.1 ± 0.2 kJ·mol^{-1}, $\Delta H^{\ddagger}$ = 101.1 ± 1.9 kJ·mol^{-1}, and $\Delta S^{\ddagger}$ = −44 ± 5 J·(K·mol)$^{-1}$, and catalyzed rearrangement of (*E*,*Z*)-**3** to **4b** gives $\Delta G^{\ddagger}$ (298 K) = 101.1 ± 0.3 kJ·mol^{-1}, $\Delta H^{\ddagger}$ = 106.1 ± 6.6 kJ·mol^{-1}, and $\Delta S^{\ddagger}$ = 17 ± 19 J·(K·mol)$^{-1}$.

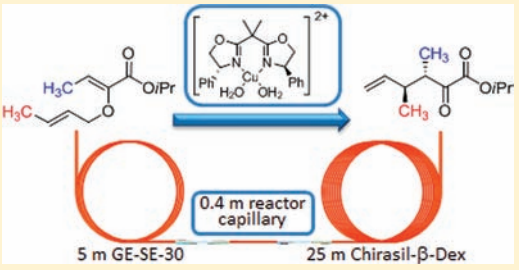

INTRODUCTION

Synthetic tools for the rapid construction of stereoisomerically pure building blocks and intermediates for target-oriented synthesis are cornerstones in the foundation of the science of synthesis. In this regard, the family of Claisen rearrangements has been particularly visible, in development as well as in application, over the past century.[1] However, catalytic asymmetric processes remained elusive until Gosteli's variation of the classical Claisen rearrangement was recognized as privileged in the development of truly catalytic asymmetric procedures.[2,3] In rapid succession, Lewis acid as well as Brønsted acid catalysts for a catalytic asymmetric Gosteli−Claisen (CAGC) rearrangement were then identified and studied mechanistically, and the CAGC rearrangement was subsequently applied in target-oriented synthesis.[4−6]

The prerequisite for improving catalytic systems and to design new catalysts is the understanding of controlling the reaction kinetics, i.e., the activation barrier in rate determining steps, by structural parameters of the catalyst and substrate.[7] Therefore the development of techniques to comprehensively investigate the reaction kinetics of a variety of substrates is of great interest. In particular the investigation of individual pathways in stereoselective reactions requires techniques to directly access enantioselectivities. Nonlinear effects arising from molecular association of enantiomers in nonracemic mixtures can cause unexpected effects, i.e., in chiroptics and NMR spectroscopy, only to mention a few.[8] Furthermore determining kinetic data of stereoselective catalyzed rearrangements can be complicated at elevated temperatures by overlaying nonstereoselective thermal conversions and even more so when observing competing reactions or isomerization of stereoisomeric reactants, e.g., the double-bond diastereomers of 2-alkoxycarbonyl-substituted allyl vinyl ethers.

Conventional reaction monitoring of crude reactant−product mixtures by decoupled catalysis and analysis employing enantioselective gas chromatography leads to apparent kinetic data with a major contribution of the thermal rearrangement. To determine the enantiomeric excess of the reaction product in such reactions, purification prior to enantioselective GC analysis is necessary and limits performing time-dependent measurements.[4] Furthermore, complete separation of the catalyst from the reaction mixture at defined reaction times to stop catalysis is imprecise.[9] Recently, microreactors based on chips[10] were successfully applied in reaction screening, however reaction and analysis are still decoupled, and therefore time-dependent reaction progress measurements are necessary. Here, we demonstrate for the first time that integration of stereoselective catalysis and stereoselective chromatography is

Received: January 1, 2011
Published: September 14, 2011

dx.doi.org/10.1021/ja207091x | *J. Am. Chem. Soc.* 2011, 133, 16444–16450

Scheme 1. Equilibria in a Chromatographic Theoretical Plate[a]

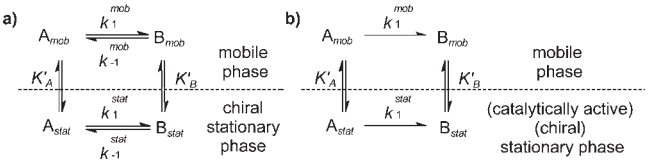

[a] Considering (a) reversible reactions (dynamic chromatography) and (b) irreversible reactions taking place in the mobile phase (mob) and stationary phase (stat). If the reaction proceeds only in the presence of a catalyst, then the reaction in the mobile phase can be neglected in scheme (b). k_1 and k_{-1} represent the forward and backward reaction rate constants in the mobile (mob) and stationary (stat) phases, and K denotes the distribution constant.

possible and constitutes a valuable tool to rapidly access reaction kinetics and selectivities with high precision, because already one single experiment using minute amounts of reactants allows determining the reaction rate constant at a given temperature and under constant reaction conditions. This increases the sample throughput, makes high-throughput reaction kinetics measurements feasible, and improves accuracy and repeatability. The technique presented here is an evolvement of on-column reaction gas chromatography (ocRGC)[11] and enantioselective dynamic chromatography,[12] which is commonly used as a highly versatile tool to investigate the stereodynamics of stereolabile compounds in thermally equilibrated mixtures of stereoisomers. In enantioselective dynamic chromatography peak profiles are characterized by a distinct plateau formation between the separated stereoisomers due to molecular interconversion. Originally, the occurrence of characteristic peak profiles has been predicted for nitrogen invertomers[13] and was later observed and used to estimate the reaction rate constants for the enantiomer separation of 1-chloro-2,2-dimethylaziridine on nickel(II) bis-[(3-heptafluorobutanoyl)-(1*R*)-camphorate] by complexation GC[14] and of 1-isopropyl-3,3-dimethyldiaziridine and 1,2,3,3-tetramethyldiaziridine on permethyl-α-cyclodextrin by inclusion GC.[15]

The interconversion of stereoisomers or reversible reaction taking place during a separation process can be illustrated by the theoretical plate model of chromatography considering every theoretical plate of multicompartmental column with N theoretical plates as chemical reactor (cf. Scheme 1a),[16] where the following three steps (i, ii, and iii) are repeatedly performed in each consecutive plate: (i) distribution of the stereoisomers A and B between mobile phase (mob) and the stationary liquid phase (stat); (ii) reversible interconversion the stereoisomers during the residence time $\Delta t = t_M/N$ (hold-up time t_M); and (iii) shifting the content of the mobile phase to the subsequent theoretical plate, whereas the content of the stationary phase is retained. In the case of irreversible reactions, i.e., irreversible rearrangements, the reaction scheme is simplified (cf. Scheme 1b), and for catalyzed reactions, the contribution of the reaction in the mobile phase can be neglected. It has to be noted that in the past, determination of reaction rate constants from such experiments was extremely time-consuming and computationally expensive.[17]

The derivation of theoretical models and equations to directly access reaction rate constants from such experiments, such as the unified equation of dynamic chromatography,[18] made the kinetic investigations presented here feasible. Conversions of reactants to reaction products can be described by the stochastic model,[19]

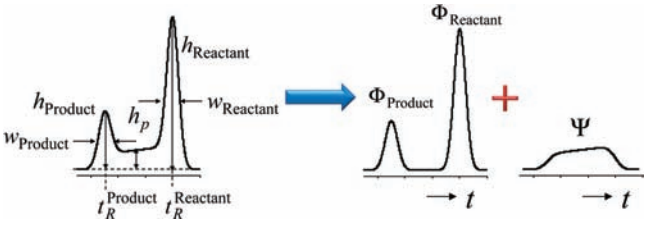

Figure 1. Mathematical separation of dynamic and on-column reaction chromatographic elution profiles into noninterconverted peaks, represented by time-dependent Gaussian distribution functions $\Phi A(t)$ and $\Phi B(t)$, and the interconverted part, represented by the stochastic distribution functions $\Psi(t)$. Here, the later eluted compound is converted into the first eluted compound during the time scale of partitioning.

Scheme 2. CAGC Rearrangement Studied by Enantioselective ocRGC

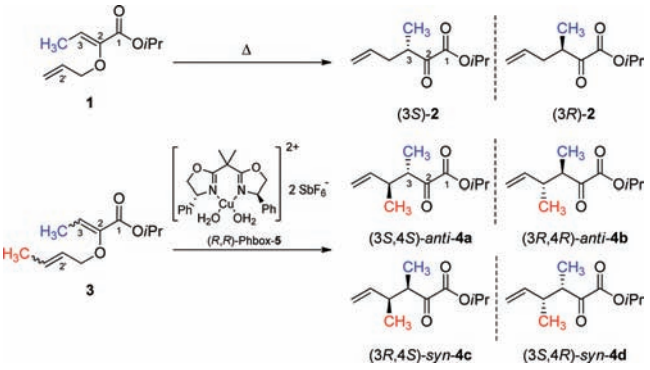

which is based on Gaussian distribution functions of the non-(inter)converted reactants and products $\Phi(t)$ and uses a time-dependent probability density function $\Psi(t)$ to describe the converted reactants (cf. Figure 1).

Applying the unified equation of chromatography allows obtaining reaction rate constants of any first-order reaction straight from chromatographic elution profiles without the need of performing reaction progress analysis. This dramatically accelerates temperature-dependent kinetic measurements and makes rapid determination of reaction kinetics feasible, as the analysis time no longer limits the rate of measurements. Detailed kinetic data and activation parameters are of great importance to model and predict activities and selectivities by computational methods.

In the following, we exemplify the power and the modes of operation of this new technique by the investigation of the uncatalyzed and catalyzed asymmetric Gosteli–Claisen rearrangement of the allyl vinyl ethers **1** and **3** by enantioselective ocRGC (cf. Scheme 2).

RESULTS AND DISCUSSION

Kinetic Studies by ocRGC of the Uncatalyzed Gosteli–Claisen Rearrangement of (*Z*)-1. The enantiomers of the α-keto ester **2** (cf. Scheme 2) can be separated with excellent resolution and selectivity by enantioselective GC in presence of the chiral stationary phase (CSP) Chirasil-β-Dex.[20] It was observed that the allyl vinyl ether **1** already undergoes the uncatalyzed

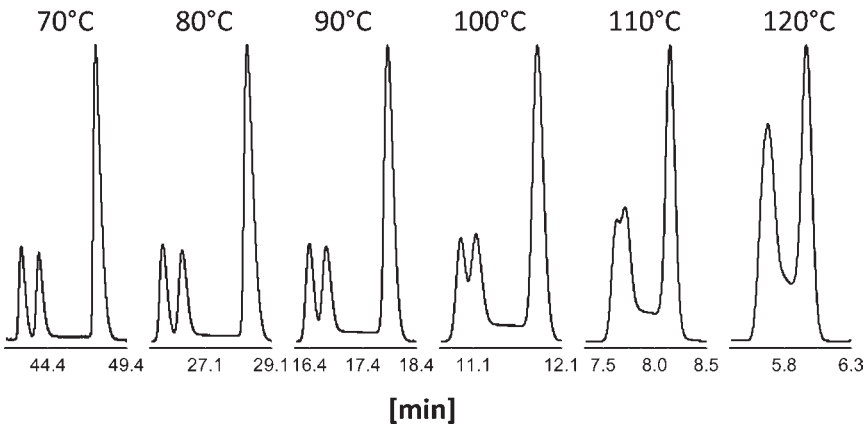

Figure 2. Elution profiles between 70 and 120 °C of enantioselective ocRGC of the uncatalyzed Gosteli−Claisen rearrangement of (*Z*)-**1** (last eluted peak) to (±)-**2** (first two eluted peaks) in presence of the CSP Chirasil-β-Dex (length, 25 m; I.D., 250 μm; film thickness, 500 nm). Helium was used as inert carrier gas at 120 kPa inlet pressure. The elution profiles are characterized by a distinct plateau formation indication the conversion of **1** to **2**.

Table 1. Summarized Results of the Uncatalyzed Gosteli−Claisen Rearrangement of (*Z*)-1 to (±)-2 Obtained by Enantioselective ocRGC (inlet pressure 120 kPa He) in Presence of the CSP Chirasil-β-Dex[a]

T [°C]	h_p (%)	(*Z*)-**1** (%)	(±)-**2** (%)	N_1	N_2	k_1 (10^{-4} s^{-1})	$\Delta G^{\ddagger}(T)$ (kJ·mol^{-1})
70.0	1.1	65.7	34.3	101 500	24 700	0.14	116.2
80.0	2.0	64.2	35.8	84 100	28 400	0.46	116.3
90.0	3.1	62.7	37.3	58 500	29 300	1.12	117.0
100.0	5.5	60.3	39.7	39 200	27 700	2.85	117.4
110.0	10.3	57.1	43.0	19 200	22 200	6.84	117.9
120.0	21.8	51.8	48.2	6800	12 500	15.56	118.3

[a] Measurements were repeated at least three times at each temperature.

Gosteli−Claisen rearrangement during enantioselective GC analysis at moderate temperatures, which is visible by a distinct plateau formation between the peaks of the enantiomers **2** and the starting substrate **1**. The identity of the peaks has been proved by coinjection of substrate **1**, racemic **2**, and by GC-MS analysis, comparing fragmentation patterns of reference spectra (cf. Supporting Information). The presence of substrate **1** complicates determination of enantiomeric excesses in conventional reaction progress analysis,[21] because of the competing thermal background rearrangement during analysis, which diminishes the true *ee* value and furthermore influences the enantiomer separation by decreasing the resolution *R*. With increasing separation temperatures between 70 and 120 °C, the plateau formation clearly increases, while the time scale of separation and enantioselectivity of the separation decreases (cf. Figure 2).

The here depicted experiments were evaluated with the unified equation (cf. Supporting Information),[18a] which allows precise and fast access to dynamic elution profiles characterized by a distinct plateau formation and partially overlapping peaks, even with different response factors of the detection system.[18d] The analytical solutions of the unified equation are implemented in the DCXplorer software package,[22] which allows to perform real time kinetic analysis of experimental data. An irreversible first-order reaction was considered, because the area under the plateau consists only of racemic compound **2**, which is corroborated by analysis of the GC-MS trace.[23] Response factors for compounds **1** and **2** are equal, and for kinetic analysis, it was taken into account that the observed peaks of the enantiomers of compound **2** are formed in the hot injector, while the racemate under the plateau is formed during the separation process. This was also proven by varying the injector temperature, which gives increasing amounts of racemate **2** with increasing temperatures and finally at 250 °C disappearance of compound **1** due to complete conversion. Mean values of the kinetic data obtained from these experiments are summarized in Table 1 (complete listing of raw data is depicted in Table S1, Supporting Information).

The Gibbs free activation energies $\Delta G^{\ddagger}(T)$ were calculated according to the Eyring eq 1 with k_B as the Boltzmann constant ($k_B = 1.380662 \times 10^{-23}$ J·K^{-1}), T as the reaction temperature [K], $\hbar$ as Planck's constant ($\hbar = 6.62617 \times 10^{-34}$ J·s), and R as the gas constant ($R = 8.31441$ J·K^{-1}·mol^{-1}). The statistical factor κ was set to 1.0.

$$\Delta G^{+}(T) = -RT\ln\left(\frac{k_1\hbar}{\kappa k_B T}\right) \quad (1)$$

Activation parameters were calculated from temperature-dependent measurements between 70 and 120 °C. The activation enthalpy $\Delta H^{\ddagger}$ of the reaction was obtained from the slope and the activation entropy $\Delta S^{\ddagger}$ from the intercept of the Eyring plot ($\ln(k_1/T)$ as a function of T^{-1}) (cf. Figure 3).

Deviations of the activation parameters $\Delta H^{\ddagger}$ and $\Delta S^{\ddagger}$ have been calculated by analysis of the confidence interval of the linear regression with a level of confidence of 95%.

Thermal rearrangement of **1** to (±)-**2** gives $\Delta G^{\ddagger}$ (298 K) = 114.1 ± 0.2 kJ·mol^{-1}, $\Delta H^{\ddagger}$ = 101.1 ± 1.9 kJ·mol^{-1}, and

$\Delta S^{\ddagger} = -44 \pm 5\ \mathrm{J \cdot (K \cdot mol)^{-1}}$ (agreement factor $r = 0.999$; residual standard deviation $s_y = 0.074$).

Kinetic Studies by ocRGC of the CAGC Rearrangement of (*E*,*Z*)-3 and (*Z*,*E*)-3. In order to extend the ocRGC[11] to the CAGC rearrangement, a second experimental setup was designed. Here, catalytically active separation columns are used as microcapillary reactors and are subsequently coupled with enantioselective separation columns to perform analysis of the reaction products. Therefore the inner surface of fused-silica capillaries (I.D. 250 μm) was coated with [Cu{(*R*,*R*)-Ph-box}](SbF$_6$)$_2$ (*R*,*R*)-**5**[24] dissolved in an inert polysiloxane matrix (ABCR PS086 containing 12−15% diphenylsiloxy and 85−88% dimethylsiloxy groups; 2, 5, 7, and 15% (w/w) catalyst loading; and film thickness of 250 nm) and using these capillaries as on-column microreactor in a GC, which allows to control reaction temperatures with high precision. Furthermore fused-silica capillaries show excellent heat-transfer properties, which is essential to study reactions under exact isothermal conditions. It has to be pointed out that the catalyst [Cu{(*R*,*R*)-Ph-box}](SbF$_6$)$_2$ (*R*,*R*)-**5** is completely dissolved in the viscous polysiloxane, representing fully homogeneous reaction conditions. The experimental setup consists of the catalytically active capillary coupled between a preseparation capillary (GE-SE-30; length, 5 m; I.D., 250 μm; film thickness, 500 nm) and an enantioselective separation capillary (CSP Chirasil-β-Dex; length, 25 m; I.D., 250 μm; and film thickness, 500 nm). The preseparation column allows thermal equilibration, a spatial separation of the injected reactants, and in particular removes impurities, which is essential to study reactions without interference of catalytically active impurities. Spatial separation of the reactants enables even investigations of compound libraries and therefore high-throughput kinetic investigations feasible, as competing reactions are excluded. The enantioselective separation column separates stereoisomeric reactants and products to determine conversions and selectivities. The advantage of this experimental setup is that experiments can be easily performed with or without the catalytically active capillary, which allows the precise determination of contact times and testing of separation selectivities at the same time. These capillaries are installed in a GC-MS (quadrupole- ion trap MS), which permits identification and quantification of reactants and products at the same time. The suitable temperature range to perform the here investigated Gosteli−Claisen rearrangement and to achieve an excellent stereoisomer separation of the reaction products was determined to be between 65 and 85 °C using helium as inert carrier gas at an inlet pressure of 220 kPa.

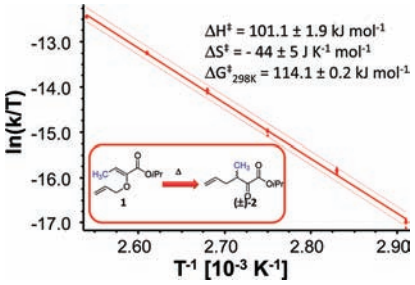

Figure 3. Eyring plot to determine activation parameters of the uncatalyzed Gosteli−Claisen rearrangement of (*Z*)-**1** to (±)-**2** obtained by temperature-dependent measurements using stereoselective ocRGC between 70 and 120 °C. The upper and lower curves represent the confidence interval of the linear regression with a level of confidence of 95%. Twenty-two data points each were considered in the linear regression.

In order to study the CAGC rearrangement of (*E*,*Z*)- and (*Z*,*E*)-**3**[25] by ocRGC, these allyl vinyl ethers were injected onto the described capillary arrangement with (cf. Figure 4d) or without (cf. Figure 4a) the catalytically active capillary column. The GC injector temperature was set to 175 °C, thus preventing a complete uncatalyzed rearrangement within the injection port. A priori, the uncatalyzed Gosteli−Claisen rearrangement of either (*E*,*Z*)- or (*Z*,*E*)-**3** may provide a mixture of the four stereoisomers (±)-*anti*- and (±)-*syn*-**4**. Experimental results,[25] in accordance with theoretical studies,[26] indicate a strong preference for a concerted bond reorganization process via a chair-like transition-state geometry for the Gosteli−Claisen rearrangement and, accordingly, the exclusive formation of (±)-anti-**4** from (*E*,*Z*)- or (*Z*,*E*)-**3** was detected by ocRGC in the absence of the catalytically active reaction capillary (cf. Figure 4b and c).

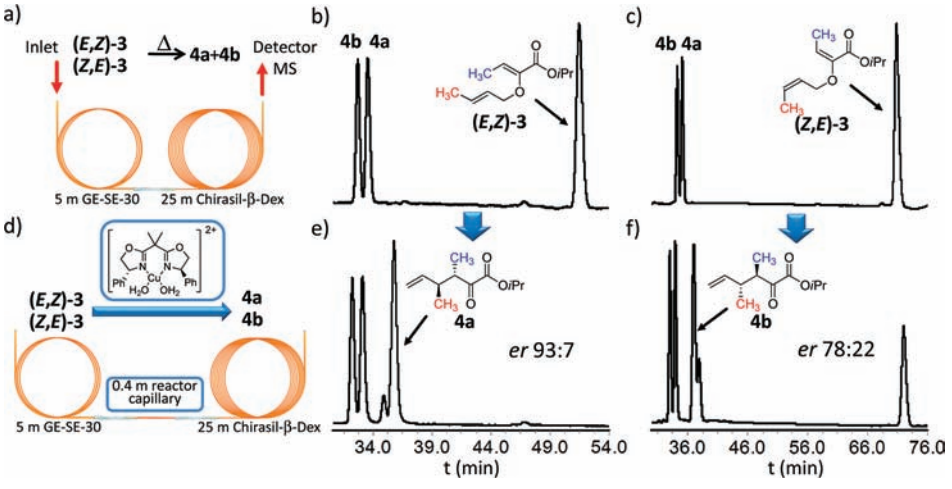

Figure 4. Experimental setup of the stereoselective on-column gas chromatographic experiment to investigate the CAGC rearrangement of (*E*,*Z*)- and (*Z*,*E*)-**3** in presence of the Lewis acid catalyst (*R*,*R*)-**5** dissolved in an inert polysiloxane matrix to form the corresponding α-keto isopropyl esters **4a** and **4b**, respectively. (b, c, e, and f) Representative chromatograms of the on-column experiment. Reaction conditions: preseparation capillary (GE-SE-30; length, 5 m; I.D., 250 μm; film thickness, 250 nm), enantioselective separation capillary (CSP Chirasil-β-Dex; length, 25 m; I.D., 250 μm; film thickness, 500 nm), reactor capillary (length, 0.4 m; I.D., 250 μm; film thickness, 250 nm), oven temperature (reaction temperature) 80 °C; inlet temperature 175 °C, and inlet pressure 220 kPa He as inert carrier gas.

dx.doi.org/10.1021/ja207091x |*J. Am. Chem. Soc.* 2011, 133, 16444–16450

Table 2. Conversions and Selectivities for the CAGC Rearrangement of (*E*,*Z*)- and (*Z*,*E*)-3 as Determined by ocRGC

entry	substrate	T (°C)	(*R*,*R*)-**5** (%)	product	conversion (%)	*er* (%)
1	(*E*,*Z*)-**3**	65	7	**4a**	>99	92:8
2	(*E*,*Z*)-**3**	80	7	**4a**	>99	93:7
3	(*Z*,*E*)-**3**	80	5	**4b**	<1	80:20
4	(*Z*,*E*)-**3**	65	7	**4b**	29	80:20
5	(*Z*,*E*)-**3**	80	7	**4b**	54	83:17
6	(*Z*,*E*)-**3**	65	15	**4b**	84	79:21
7	(*Z*,*E*)-**3**	80	15	**4b**	97	78:22

In contrast to substrate **1**, uncatalyzed formation of the rearrangement product from (*E*,*Z*)- or (*Z*,*E*)-**3** during the time-scale of separation was not detectable by highly sensitive MS measurements, and no characteristic plateau formation was observable in the here investigated temperature range.

Next, the reactor capillary with the embedded catalyst (*R*,*R*)-**5** was coupled between the preseparation and enantioselective separation capillary (cf. Figure 4d). Using this experimental setup, the diastereo- and enantioselective formation of **4a** from (*E*,*Z*)-**3** and **4b** from (*Z*,*E*)-**3** was detected (cf. Figure 4e and f). The advantage of this approach is that the enantiomeric rearrangement products **4a** and **4b**, formed by the uncatalyzed rearrangement in the injector, can be used as internal standard to determine contact times Δt of the reactants and the catalytically active capillary. The enantiomeric products from the catalyzed rearrangement are eluted with a time delay compared to the racemate formed by the uncatalyzed background reaction, because of the separation of the reactants (*E*,*Z*)- and (*Z*,*E*)-**3** from the noncatalytically formed product by the achiral preseparation column. Reaction products **4** show less retention compared to the reactant in presence of the achiral stationary phase GE-SE-30 and Chirasil-β-Dex.

From these chromatographic data conversions of the individual stereoisomers, *er* values and, consequently, the catalytic activity can be precisely determined (cf. Table 2).

The embedded catalyst (*R*,*R*)-**5** provides excellent conversions and *er* values for the CAGC rearrangement of (*E*,*Z*)-**3** to **4a**, and notably, the catalyst maintains its activity and selectivity within the investigated temperature range between 65 and 85 °C. We also investigated the stability of the catalyst by performing a series of substrate injections. It was found that the activity decreases over the first six injections and then stays at a stable activity level, while the enantioselectivity is unchanged (cf. Figure S24, Supporting Information). The conversion of the reactants and hence the catalytic activity of the embedded catalyst (*R*,*R*)-**5** correlates with its concentration, (cf. Figure S26, Supporting Information), however it has to be noted that for low catalyst loadings, only very low activities were detectable, which can be attributed to surface silanol groups of the fused capillary and silanol end groups of the polysiloxane PS086.

In comparison to the conversion of (*E*,*Z*)-**3** to **4a**, the conversion of (*Z*,*E*)-**3** to **4b** is noticeably slower, and the enantioselectivity is decreased. Kinetic data and enantioselectivities obtained by enantioselective ocRGC agree very well with data obtained by independent methods reported in literature.[4d,25,26]

Determination of Activation Parameters of the Catalytic Asymmetric Gosteli–Claisen (CAGC) Rearrangement of (*E*,*Z*)-3 and (*Z*,*E*)-3. To obtain experimental activation parameters $\Delta H^{\ddagger}$ and $\Delta S^{\ddagger}$ of the CAGC rearrangement catalyzed by (*R*,*R*)-**5**, the incomplete conversion of (*Z*,*E*)-**3** to **4a** and **4b** was investigated by temperature-dependent measurements between 65 and 85 °C in detail. Best agreement in the calculation of reaction rate constants was achieved by application of a pseudo-first-order reaction rate law, as described in literature,[5c] for parallel reactions, where both pathways yield the enantiomeric reaction products **4a** and **4b** (cf. Supporting Information). Integrated peak areas can be directly used to determine reaction kinetics, because the flame ionization detector (FID) gives the same signal intensities for constitutional isomers. Contact times Δt are calculated from measurements with and without the catalytically active column, which are performed at various temperatures and inlet pressures.[11] Furthermore comparison of the dynamic with the static ocRGC mode allows to independently validating kinetic data obtained by these experiments. The Gibbs free activation energies $\Delta G^{\ddagger}(T)$ were calculated according to the Eyring equation by setting the statistical transmission factor κ to 1. $\Delta G^{\ddagger}$ at 80 °C was determined to be 100.2 ± 0.3 kJ·mol^{-1} for the rearrangement of (*Z*,*E*)-**3** to the major enantiomer **4b** and 104.2 ± 0.3 kJ·mol^{-1} for the rearrangement of (*Z*,*E*)-**3** to the minor enantiomer **4a**. The high activity and stereoselectivity of the CAGC rearrangement catalyzed by (*R*,*R*)-**5** compared to the uncatalyzed reaction are corroborated by the activation parameters determined for the formation of the individual enantiomers. The activation enthalpy $\Delta H^{\ddagger}$ of the reaction was obtained from the slope and the activation entropy $\Delta S^{\ddagger}$ from the intercept of the Eyring plot ($\ln(k/T)$ as a function of T^{-1}). Rearrangement of (*Z*,*E*)-**3** to **4b** in the presence of (*R*,*R*)-**5** gives $\Delta H^{\ddagger}$ = 106.1 ± 6.6 kJ·mol^{-1} and $\Delta S^{\ddagger}$ = 17 ± 19 J·(K·mol)$^{-1}$, and (*Z*,*E*)-**3** to **4a** gives $\Delta H^{\ddagger}$ = 106.9 ± 12.3 kJ·mol^{-1} and $\Delta S^{\ddagger}$ = 8 ± 35 J·(K·mol)$^{-1}$ (cf. Figure 5). Deviations of the activation parameters $\Delta H^{\ddagger}$ and $\Delta S^{\ddagger}$ have been calculated by analysis of the confidence interval of the linear regression with a level of confidence of 95%, giving agreement factors of r = 0.986 and 0.956 and residual standard deviations of s_y = 0.450 and 1.532, respectively. It has to be pointed out that the here employed approach makes the investigation of single isomeric reactants possible, because even traces of isomers or isomerized reactants are removed by the first separation dimension, which would not make kinetic analysis at high precision feasible.

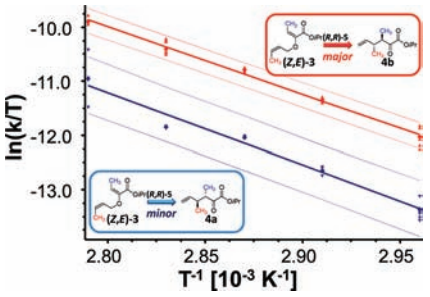

Figure 5. Eyring plot to determine activation parameters of the CAGC rearrangement of (*Z*,*E*)-**3** to **4a** and **4b** obtained by temperature-dependent measurements using stereoselective ocRGC between 65 and 85 °C. For experimental parameters see Figure 4. The upper and lower curves represent the confidence intervals of the linear regression with a level of confidence of 95%. Thirty-two data points each were considered in the linear regression.

These activation parameters show that the activation enthalpy $\Delta H^{\ddagger}$ and activation entropy $\Delta S^{\ddagger}$ is lowered by $\Delta\Delta H^{\ddagger}$ = 0.8 kJ·mol^{-1} and $\Delta\Delta S^{\ddagger}$ = 9 J·(K·mol)$^{-1}$, respectively, which

indicates that the transition state for the formation of **4a** compared to the formation of **4b** is less favored. Surprisingly, these investigations by ocRGC reveal also that the CAGC rearrangement proceeds even at elevated temperatures with excellent selectivity at increased conversion rates, which makes this reaction highly efficient and attractive for larger scale chemical processes.

CONCLUSIONS

As demonstrated here, we are the first to show that integration of stereoselective catalysis and direct analysis of the reactants in an on-column chromatographic reactor is a highly versatile and powerful tool to study stereoselective reactions starting from stereoisomeric reactants and to distinguish from nonstereoselective thermal processes. Detailed and precise high-throughput kinetic studies are feasible because in comparison to conventional progress kinetic analysis, reaction rate constants are directly accessible from the enantioselective ocRGC experiments. Furthermore competing and possible side reactions can be simultaneously investigated under exactly the same reaction conditions, because of the preseparation of the reactants. Additionally, the employed experimental setup simultaneously yields important kinetic information to optimally tune reaction conditions. Other advantages of this technique are the lower consumption of reagents, as large excesses can be avoided, the drastically reduced time frame of the experiment, and the higher enantiomeric excess of the performed reaction compared to conventional experiments.

ASSOCIATED CONTENT

Supporting Information. Experimental setup, spectroscopic data, NMR and MS spectra of all compounds, complete procedures, and complete kinetic analysis. This material is available free of charge via the Internet at http://pubs.acs.org.

AUTHOR INFORMATION

Corresponding Author
trapp@oci.uni-heidelberg.de

ACKNOWLEDGMENT

J.R. and M.H. express their gratitude to the Deutsche Forschungsgemeinschaft (HI 628/3) and the Technische Universität Dortmund for financial support. J.T. and O.T. thank the Deutsche Forschungsgemeinschaft (DFG) for financial support of this research (SFB 623 'Molecular Catalysts: Structure and Functional Design').

REFERENCES

(1) *The Claisen Rearrangement*; Hiersemann, M., Nubbemeyer, U., Eds. Wiley-VCH: Weinheim, Germany, 2007.

(2) For recent reviews on catalyzed Claisen rearrangements, see: (a) Hiersemann, M.; Abraham, L. *Eur. J. Org. Chem.* **2002**, 1461–1471. (b) Majumdar, K. C.; Alam, S.; Chattopadhyay, B. *Tetrahedron* **2008**, *64*, 597–643.

(3) Gosteli, J. *Helv. Chim. Acta* **1972**, *55*, 451–460.

(4) For the development of Lewis acid catalysts, see: (a) Hiersemann, M. *Synlett* **1999**, 1823–1825. (b) Hiersemann, M.; Abraham, L. *Org. Lett.* **2001**, *3*, 49–52. (c) Abraham, L.; Czerwonka, R.; Hiersemann, M. *Angew. Chem., Int. Ed.* **2001**, *40*, 4700–4703. (d) Abraham, L.; Körner, M.; Schwab, P.; Hiersemann, M. *Adv. Synth. Catal.* **2004**, *346*, 1281–1294. (e) Abraham, L.; Körner, M.; Hiersemann, M. *Tetrahedron Lett.* **2004**, *45*, 3647–3650. For a computational study, see: (f) Öztürk, C.; Balta, B.; Aviyente, V.; Vincent, M. A.; Hillier, I. H. *J. Org. Chem.* **2008**, *73*, 4800–4809.

(5) For the development of Brønsted acid catalysts, see: (a) Kirsten, M.; Rehbein, J.; Hiersemann, M.; Strassner, T. *J. Org. Chem.* **2007**, *72*, 4001–4011. (b) Uyeda, C.; Jacobsen, E. N. *J. Am. Chem. Soc.* **2008**, *130*, 9228–9229. (c) Uyeda, C.; Jacobsen, E. N. *J. Am. Chem. Soc.* **2011**, *133*, 5062–5075.

(6) For selected applications of the catalytic asymmetric Gosteli–Claisen rearrangement in target-oriented synthesis, see: (a) Pollex, A.; Hiersemann, M. *Org. Lett.* **2005**, *7*, 5705–5708. (b) Körner, M.; Hiersemann, M. *Org. Lett.* **2007**, *9*, 4979–4982. (c) Gille, A.; Hiersemann, M. *Org. Lett.* **2010**, *12*, 5258–5261.

(7) Campbell, C. T. *Nature* **2004**, *432*, 282–283.

(8) (a) Puchot, C.; Samuel, O.; Dunach, E.; Zhao, S.; Agami, C.; Kagan, H. B. *J. Am. Chem. Soc.* **1986**, *108*, 2353–2357. (b) Girard, C.; Kagan, H. B. *Angew. Chem., Int. Ed.* **1998**, *37*, 2923–2959. (c) Girard, C.; Kagan, H. B. *Can. J. Chem.* **2000**, *78*, 816–828. (d) Kagan, H. B. *Synlett, Special issue* **2001**, 888–899. (e) Blackmond, D. G. *Acc. Chem. Res.* **2000**, *33*, 402–411. (f) Reetz, M. T.; Fu, Y.; Meiswinkel, A. *Angew. Chem., Int. Ed.* **2006**, *45*, 1412–1415. (g) Satyanarayana, T.; Abraham, S.; Kagan, H. B. *Angew. Chem., Int. Ed.* **2009**, *48*, 456–494.

(9) Trapp, O. *J. Chromatogr., A* **2008**, *1184*, 160–190.

(10) (a) Burns, M. A.; Johnson, B. N.; Brahmasandra, S. N.; Handique, K.; Webster, J. R.; Krishnan, M.; Sammarco, T. S.; Man, P. M.; Jones, D.; Heldsinger, D.; Mastrangelo, C. H.; Burke, D. T. *Science* **1998**, *282*, 484–487. (b) Watts, P.; Haswell, S. J. *Chem. Soc. Rev.* **2005**, *34*, 235–246. (c) Baxendale, I. R.; Deeley, J.; Griffiths-Jones, C. M.; Ley, S. V.; Saaby, S.; Tranmer, G. K. *Chem. Commun.* **2006**, 2566–2568. (d) Belder, D.; Ludwig, M.; Wang, L. -W.; Reetz, M. T. *Angew. Chem.* **2006**, *118*, 2523–2526. *Angew. Chem., Int. Ed.* **2006**, *45*, 2463–2466. (e) de Mello, A. J. *Nature* **2006**, *442*, 394–402. (f) Abdallah, R.; Fumey, B.; Meille, V.; de Bellefon, C. *Catal. Today* **2007**, *125*, 34–39. (g) Sahoo, H. R.; Kralj, J. G.; Jensen, K. F. *Angew. Chem.* **2007**, *119*, 5806–5810. *Angew. Chem., Int. Ed.* **2007**, *46*, 5704–5708. (h) Ceylan, S.; Friese, C.; Lammel, C.; Mazac, K.; Kirschning, A. *Angew. Chem.* **2008**, *120*, 9083–9086. (i) Wang, N.; Matsumoto, T.; Ueno, M.; Miyamura, H.; Kobayashi, S. *Angew. Chem.* **2009**, *121*, 4838–4840. *Angew. Chem., Int. Ed.* **2009**, *48*, 4744–4746. (j) Valera, F. E.; Quaranta, M.; Moran, A.; Blacker, J.; Armstrong, A.; Cabral, J. T.; Blackmond, D. G. *Angew. Chem.* **2010**, *122*, 2530–2537. *Angew. Chem., Int. Ed.* **2010**, *49*, 2478–2485.

(11) Trapp, O.; Weber, S. K.; Bauch, S.; Hofstadt, W. *Angew. Chem.* **2007**, *119*, 7447–7451. *Angew. Chem., Int. Ed.* **2007**, *46*, 7307–7310. (b) Trapp, O.; Weber, S. K.; Bauch, S.; Bäcker, T.; Hofstadt, W.; Spliethoff, B. *Chem.—Eur. J.* **2008**, *14*, 4657–4666. (c) Weber, S. K.; Bremer, S.; Trapp, O. *J. Chem. Eng. Sci.* **2010**, *65*, 2410–2416. (d) Lang, C.; Gärtner, U.; Trapp, O. *Chem. Commun.* **2011**, *47*, 391–393.

(12) (a) Trapp, O.; Schoetz, G.; Schurig, V. *Chirality* **2001**, *13*, 403–414. (b) Krupcik, J.; Oswald, P.; Majek, P.; Sandra, P.; Armstrong, D. W. *J. Chromatogr., A* **2003**, *1000*, 779–800. (c) Wolf, C. *Chem. Soc. Rev.* **2005**, *34*, 595–608. (d) D'Acquarica, I.; Gasparrini, F.; Pierini, M.; Villani, C.; Zappia, G. *J. Sep. Sci.* **2006**, *29*, 1508–1516. (e) Wolf, C. *Dynamic Stereochemistry of Chiral Compounds - Principles and Applications*; RSC Publishing: Cambridge U.K., 2008.

(13) Schurig, V.; Leyrer, U. *Tetrahedron: Asymmetry* **1990**, *1*, 865–868.

(14) (a) Schurig, V.; Bürkle, W. *J. Am. Chem. Soc.* **1982**, *104*, 7573–7580. (b) Bürkle, W.; Karfunkel, H.; Schurig, V. *J. Chromatogr.* **1984**, *288*, 1–14.

(15) Jung, M.; Schurig, V. *J. Am. Chem. Soc.* **1992**, *114*, 529–534.

(16) (a) Martin, A. J. P.; Synge, R. L. M. *Biochem. J.* **1941**, *35*, 1358–1368. (b) Craig, L. C. *J. Biol. Chem.* **1944**, *155*, 519–534. (c) Kallen, J.; Heilbronner, E. *Helv. Chim. Acta* **1960**, *43*, 489–500.

(17) (a) Trapp, O.; Schurig, V. *Comput. Chem.* **2001**, *25*, 187–195. (b) Trapp, O. *J. Chem. Inf. Comput. Sci.* **2004**, *44*, 1671–1679.

(18) (a) Trapp, O. *Anal. Chem.* **2006**, *78*, 189–198. (b) Trapp, O. *Electrophoresis* **2006**, *27*, 534–541. (c) Trapp, O. *Chirality* **2006**, *18*, 489–497. (d) Trapp, O.; Bremer, S.; Weber, S. K. *Anal. Bioanal. Chem.* **2009**, *395*, 1673–1679.

(19) (a) Keller, R. A.; Giddings, J. C. *J. Chromatogr.* **1960**, *3*, 205–220. (b) Dondi, F.; Cavazzini, A.; Remelli, M. *Adv. Chromatogr.* **1998**, *38*, 51–70.
(20) (a) Schurig, V.; Schmalzing, D.; Schleimer, M. *Angew. Chem.* **1991**, *103*, 994–996. *Angew. Chem., Int. Ed.* **1991**, *30*, 987–989. (b) Cousin, H.; Trapp, O.; Peulon-Agasse, V.; Pannecoucke, X.; Banspach, L.; Trapp, G.; Jiang, Z.; Combret, J. C.; Schurig, V. *Eur. J. Org. Chem.* **2003**, 3273–3287.
(21) Blackmond, D. G. *Angew. Chem.* **2005**, *117*, 4374–4393. *Angew. Chem., Int. Ed.* **2005**, *44*, 4302–4320.
(22) Trapp, O. *J. Chromatogr., B* **2008**, *875*, 42–47.
(23) Trapp, O. *J. Chromatogr., A* **2010**, *1217*, 1010–1016.
(24) Evans, D. A.; Scheidt, K. A.; Johnston, J. N.; Willis, M. C. *J. Am. Chem. Soc.* **2001**, *123*, 4480–4491.
(25) Rehbein, J.; Leick, S.; Hiersemann, M. *J. Org. Chem.* **2009**, *74*, 1531–1540.
(26) Rehbein, J.; Hiersemann, M. *J. Org. Chem.* **2009**, *74*, 4336–4342.